Unsteady flows in milli-and microsystems : analysis of wall shear rate fluctuations

Florian Huchet, P Legentilhomme, J Legrand, A Montillet, J Comiti

▶ **To cite this version:**

Florian Huchet, P Legentilhomme, J Legrand, A Montillet, J Comiti. Unsteady flows in milli-and microsystems : analysis of wall shear rate fluctuations. Experiments in Fluids, 2011, 51 (3), pp 597-610. 10.1007/s00348-011-1079-1 . hal-00850614

HAL Id: hal-00850614
https://hal.science/hal-00850614

Submitted on 7 Aug 2013

HAL is a multi-disciplinary open access archive for the deposit and dissemination of scientific research documents, whether they are published or not. The documents may come from teaching and research institutions in France or abroad, or from public or private research centers.

L'archive ouverte pluridisciplinaire **HAL**, est destinée au dépôt et à la diffusion de documents scientifiques de niveau recherche, publiés ou non, émanant des établissements d'enseignement et de recherche français ou étrangers, des laboratoires publics ou privés.

Exp Fluids
DOI 10.1007/s00348-011-1079-1

RESEARCH ARTICLE

Unsteady flows in milli- and microsystems: analysis of wall shear rate fluctuations

F. Huchet · P. Legentilhomme · J. Legrand · A. Montillet · J. Comiti

Received: 24 September 2010 / Accepted: 17 March 2011
© Springer-Verlag 2011

Abstract The particular benefits of microfluidic systems, in terms of heat and mass transfer enhancement, require conducting local flow diagnostics, especially when unsteady properties of the microflow can play a critical role at the reaction interface, as currently observed in the fields of bioengineering and chemical engineering. The present paper focuses on unsteady confined flows within microsystems characterized by various geometries of crossing channels and exhibiting high surface-to-volume ratios. An experimental analysis of the signal measured at microsensors embedded to the wall of microsystems is discussed. In the objective of performing flow diagnostics, including regime identification and wall flow structure recognition, two methods for electrochemical signal processing are investigated and compared within an experimental network of crossing minichannels. One method is based on the use of a transfer function, while the other, the so-called Sobolik solution (Sobolik et al. in Coll Czech Chem Commun 52:913–928, 1987), consists of finding a direct solution to the mass balance equation. Sobolik's method has been selected given its ability to provide a description, over a wide range of Reynolds numbers ($317 < Re < 3{,}535$), for all wall shear rate fluctuations, as well as for the associated mixing scales in the power spectra density (PSD). This technique is then applied to flow within micromixers composed of two crossing microchannels in order to study highly unsteady and inhomogeneous microflows. The hydraulic diameters of the studied channels are 500 and 833 μm, respectively. Two flow patterns are investigated herein: the crossing-flow type and the impinging flow (or so called co-flow) for a Reynolds number range between 173 and 3,356. The PSD of wall shear rate fluctuations reveals various flow characteristics depending on the microchannel aspect ratio.

P. Legentilhomme · J. Legrand · A. Montillet · J. Comiti
GEPEA, Université de Nantes, CNRS, UMR 6144,
C.R.T.T, 37 bd de l'Université, BP 406,
44602 Saint-Nazaire Cedex, France

F. Huchet (✉)
IFSTTAR, Department Materials, Aggregates and Materials Processing, Route de Bouaye, BP 4120,
44341 Bouguenais Cedex, France
e-mail: florian.huchet@ifsttar.fr

1 Introduction

Over the past decade, many scientific fields (e.g., chemical engineering, materials science, biology) have been especially interested in the attention generated by the scientific subject of microfluidics, which is the term used to describe the flow in devices with dimensions extending from the millimeter scale to the micrometer scale and capable of handling fluid volumes in the range of nano- to microliters. This particular field of study offers great promise in favor of designing sustainable processes. The main reason for this strong potential is the increase in the ratio of transfer surface area to fluid volume, with the effect of enhancing heat and mass transfers between solid and fluid. On the other hand, the mixing rate between two initially segregated streams is accelerated and their corresponding crossing occurs in a minimum spatial domain. These higher heat and mass fluxes at either the solid–liquid or liquid–liquid interface inside microsystems may be used for several purposes: to test hazardous reactions, to improve process design, and to apply new kinds of compact processes in industry. Fast chemical reactions have been performed inside microreactors (Kockmann et al. 2006), with an original chaotic geometry being designed for

Published online: 31 March 2011

micromixers (Hessel et al. 2005) or heat microexchangers in the presence of exothermal reactions with high heat flux densities. Various complex geometries were studied using numerical approaches or comprehensive measurements in order to characterize transfer phenomena within heat microexchangers (Brandner et al. 2006) or microreactors (Commenge et al. 2004). The installation of compact, microstructured exchangers composed of manifold microchannels is also very promising when producing large quantities of selective components (Gavrilidis et al. 2002). Many studies focusing on the hydrodynamics and mixing of fluids according to various microchannel geometries have thus been dedicated to an assessment of new equipment involved in chemical and biological transformations (Hansen and Quake 2003).

The flow regimes inside these microdevices tend to be of the transitional or turbulent type, and it is now critical to determine the optimal size of manifold microchannels in order to both reduce the pressure drop and control microflow dynamics within these milli- or microexchangers (Saber et al. 2009, 2010). Yet in this pursuit, researchers generally end up confronting a number of interdependent problems.

Despite recent advances in MEMS (microelectrical mechanical systems) technology as well as in microfabrication techniques (using silicon, glass, or polymers by means of μ-stereolithography), the typical experimental difficulties encountered relate to microsystem metrology, making measurements of global and local parameters difficult to perform and therefore difficult to reproduce in microchannels. Controlling the surface conditions and crossing section of flow passage remains a recurrent problem. Recent results (Mokrani et al. 2009) in investigating convective heat transfer flow under controlled geometric microchannel dimensions with various aspect ratios have shown that solid–fluid interface effects (i.e., wettability, charge density) do not play a significant role in the transfer phenomena (momentum and heat) inside microchannels sized larger than 50 μm. However, as mentioned by various authors (Sharp and Adrian 2004; Morini 2004), the experimental data devoted to evaluating convective heat transfer coefficients indicate scattered results (50% in magnitude) for differently shaped microchannels (circular, rectangular, trapezoidal) and for a range of hydraulic diameters (from 50 to 1,000 μm). The classical dimensionless laws used for scaling heat and mass exchangers appear to be compromised when examining compact heat and mass microexchangers. The local momentum transfer variation caused by geometric parameters of the microchannels (roughness, inlet and outlet effects, shape effects in microchannels, etc.) is the main reason for the convective transfer law non-conformity. Local flow characteristics, such as transient effects, laminar boundary layer destabilization, near-wall intermittency, entrance of undeveloped flows, inlet flow rate control, and recirculation, are manifested by the geometric properties of microdevices. These local flow disturbances are considerable with respect to the bulk flow in microsystems, as opposed to the case of more conventionally sized channels.

The characterization of local transport properties is also crucial in the case of transitional or turbulent flow regimes inside microflows. Such a characterization step helps model the microflow inside microstructured exchangers since a continuous medium mechanics approach proves to be feasible. The flows inside mini- or microchannels can actually be characterized by certain non-established properties, while transitional regimes are governed by intermittent phenomena and large structures that are elongated in the streamwise direction (Huchet et al. 2008a; Natrajan and Christensen 2009). The difficulties encountered in computational fluid dynamics for the solving of the near-wall flow are reinforced in the case of microchannels characterized by an increased surface to volume ratio. The surface area available to small fluid volumes requires a highly refined mesh in the near-wall area, where transient phenomena and large gradients occur. To summarize, numerical simulation difficulties are due to:

1. laminar instability theory, in the case of a flow regime corresponding to the initial appearance of fluctuations;
2. issues relative to the turbulent flow regime, as characterized by intermittent turbulent bursts in the near-wall location, for which few models are available.

When considering mixing at the microscale, a characterization of local flow behavior becomes essential to control mass transfer between reactants across the various micromixers and microreactors developed in the field of reaction engineering (Hessel et al. 2005). Many studies investigating flow through microsystems featuring different shapes and flow configurations have become available in the literature over the past few years. Among the topics studied, a T-shaped microchannel (Bothe and Warnecke 2006) and hydrodynamic focusing (Stroock et al. 2002) offer promising classes of flow configurations for micromixing applications. In the area of mixing research, the characterization of mixing scales appears fundamental for design and optimization of microfluidic devices. Fluid flow at the microscale pertains mainly to the scales of flow in the transitional and turbulent regimes. The conditions of stationarity, homogeneity, and isotropy cannot be assumed in confined turbulent flows within microsystems, and moreover predicting the local dissipation rate becomes a key issue for mixing control at the microscale. Academically and practically speaking, it is therefore important to study confined flow and mixing by paying special attention to small-scale motions. In spite of recent research

dedicated to a local hydrodynamics analysis inside microchannels, in particular by means of μ-PIV and μ-LIF (Hoffmann et al. 2006), very little work (Huchet et al. 2008a; Natrajan and Christensen 2009) include both hydrodynamics and mixing study at the small scale, and especially in the near-wall vicinity. A high sampling frequency is required to adequately describe a confined turbulent flow characterized by a wide fluctuations range within the energy density spectra. This issue has recently been viewed as an important challenge as regards classical turbulence investigation techniques (Lui et al. 2009).

The objective of our present work is to analyze unsteady flow properties in various configurations of miniaturized systems by relying upon electrodiffusion diagnostics in the near-wall vicinity; this method is currently employed to investigate solid–liquid mass transfer and is recognized for its ability to determine wall shear rates using microelectrodes. Mixing properties have a direct relationship with the local flow structures developing in the turbulent boundary layer. The intermittent properties of observed instabilities are closely correlated with near-wall flow. In pursuit of this objective, a few microsensors may be used to determine instantaneous wall friction. Some of the existing alternative techniques are indirect methods, such as hot film, and based on convective heat transfer between the heating element and the fluid. Implementation of an electrochemical technique appears to be an in situ method suitable for microsystems such as microfluidic facilities. Microfabrication technology, based on optical lithography, allows miniaturizing electrochemical microsensors and their integration as non-intrusive probes in the microchannel wall (Kjeang et al. 2007; Schrott et al. 2009).

This electrochemical technique was preliminarily validated in terms of mapping the fluctuating wall shear rate and characterizing liquid–solid mass transfer inside a network of crossing minichannels (Huchet et al. 2007). The network can be considered as a geometric model for studying a complex confined flow, such as the kind encountered in certain miniheat exchangers or minicatalytic reactors. Subsequently, various studies were performed that included a mixing analysis and energy dissipation in various minichannel networks (Huchet et al. 2008b).

This paper focuses on the unsteady properties of flow developing inside both mini- and microfluidics systems of rectangular cross-section and with two aspect ratios ($\gamma = 1$ and $\gamma = 0.2$), as characterized by two microchannels crossing at right angles. During an initial analysis (in Sect. 2), two electrodiffusion post-processing steps will first be compared by conducting a spectral analysis of the measured signals in a network of minichannels ($d_h = 1.5$ mm). The selected method will then be applied to the electrical current recorded on microelectrodes flush-mounted on the micromixer wall featuring different cross-sections ($d_h = 833$ µm and $d_h = 500$ µm, respectively). A previous study (Huchet et al. 2008c) was carried out within the scope of determining the mean wall shear rate for two flow configurations, i.e., crossing-flow and impinging-flow. To the best of our knowledge, the present spectral analysis of wall shear rate fluctuations inside micromixers constitutes the first experimental study to reveal the fine-scale description of wall flow at the junction location where fluid streams are stretched and sheared (Sect. 3). Conclusions from this program will be provided in Sect. 4.

2 Comparison of electrochemical flow diagnostics

2.1 Electrodiffusion technique for wall shear rate determination in a network of crossing minichannels

This technique is based on deriving a wall shear rate measurement (Hanratty and Campbell 1983), which consists of using mass transfer probes flush-mounted on the wall. A fixed potential difference is then applied between the microprobes acting as cathodes and a large-area anode. A fast electrochemical reduction reaction takes place at the microprobe surface, thus allowing the diffusion boundary layer to develop. The operating principle involves measuring a current under diffusion-limiting conditions at the microprobes in such a way that the reaction rate is diffusion-controlled through the mass transfer boundary layer, δ_d, and that ionic migration can be neglected due to the presence of a supporting electrolyte. The measured intensity varies with voltage applied between anode and cathode until reaching a constant value, I_{lim}, which corresponds to the limiting diffusion conditions. The mass transfer coefficient, k, can then be calculated by Faraday's expression as follows:

$$k = I_{lim}/v_e \Im A c_0 \tag{1}$$

where v_e is the number of electrons involved in the redox reaction, $\Im$ Faraday's constant, A the microelectrode surface area, and c_0 the bulk concentration of the reacting species.

The mean measured limiting current is controlled by convective diffusion, and the well-known Lévêque formula (Lévêque 1928) can be applied in order to determine the mean wall shear rate, $\bar{s}$. Reiss and Hanratty (1963) solved the stationary equation for a circular microelectrode and found the following relationship:

$$\bar{S} = 3.22\left(\bar{I}_{lim}\Big/ v_e \Im c_0 d_e^{5/3} D^{2/3}\right)^3 \tag{2}$$

where d_e is the diameter of the circular electrode and D is the diffusion coefficient of the active species in the solution.

The analytical, quasi-steady state interpretation solution of the measured current correctly describes the time response of the mass transfer rate, while the instantaneous wall shear rate, $s_q(t)$, can be related to the instantaneous mass transfer rate by the same equation as for steady flow (i.e., Eq. 2):

$$s_q(t) = 3.22(v_e \Im c_0)^{-3} D^{-2} d_e^{-5} I_{lim}^3(t) \quad (3)$$

The experimental set-up is depicted in Fig. 1. The network's total length H equals 105 mm and its width 52 mm; it is composed of altuglass and contains ten crossing minichannels with a square cross-section of side length 1.5 mm. A total of 39 microelectrodes with a diameter close to that of the platinum wire used, i.e., 250 μm, were placed at different locations between the system inlet and outlet. Their typical positions inside the minichannels were respectively the following: either just before (B) or after (A) a crossing, both at a crossing center (C), and midway between two microchannel (M) crossings. A bed of spheres and a nickel grid were positioned respectively at the inlet and outlet. This bed of spheres ensures an adequate distribution of flow in each inlet minichannel, while the grid acts as the anode for the electrical circuit. Details on this electrochemical technique can be found in a previous work (Huchet et al. 2007), which describes both the determination of the electrochemical species diffusion coefficient (fast redox system: ferri/ferrocyanide in its reduction step) and the microelectrode calibration method.

In the present work, three operating microelectrodes are chosen within the scope of the signal analysis performed on the instantaneous current:

- M34 (diameter: 258 μm) is located at the network inlet where the flow is not fully developed,
- A28 (diameter: 256 μm) is located in the area where flow is establishing,
- M15 (diameter: 253 μm) is located close to the network outlet.

For purposes of illustration, Fig. 2 presents the limiting diffusion current recorded at the M15 electrode for different Reynolds numbers. The corresponding quasi-steady state solution of the wall shear rate is given in Fig. 3. For high-frequency fluctuations of the wall shear rate, the filtering effect of the mass boundary layer dampens mass transfer rate fluctuations, and the quasi-steady state solution is not representative. The cutoff frequency under which the quasi-steady state can be considered valid is rather low, as a result of the high value of the Schmidt number in the electrolyte ($Sc \approx 1{,}700$).

Determining the transfer function has been the objective of several studies (Deslouis et al. 1990; Nakoryakov et al. 1986). This function allows identifying wall shear stress dynamics. A second method, based on Sobolik's correction (Sobolik et al. 1987), takes into account calculation of the wall shear stress evolution over time. An application and comparison of these two methods in a minichannel network will be discussed in the next subsection.

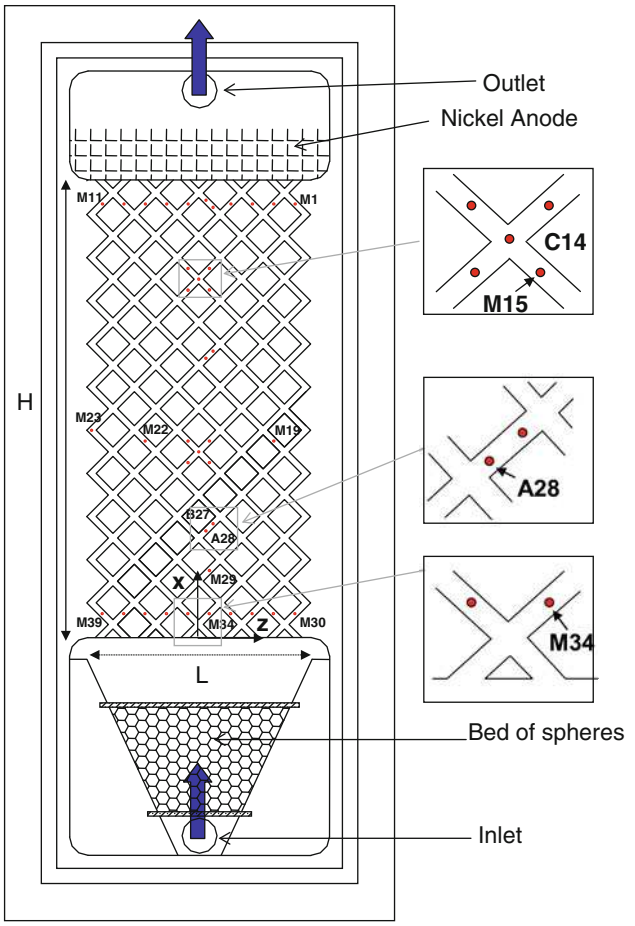

Fig. 1 Experimental network of crossing minichannels

2.2 Unsteady flow diagnostics from wall shear rate fluctuations

2.2.1 *Sobolik's correction*

This method is based on correcting the dynamic behavior of the probe through introducing the diffusion–convection equation solution proposed by Sobolik et al. (1987). These authors solved the mass balance equation by assuming that the concentration field was a similar function of three variables as follows:

$$C(x, y, t) = c_0 f(\eta) \quad (4)$$

$$\eta = y f(t)^{1/3} / \delta_d(x) \quad (5)$$

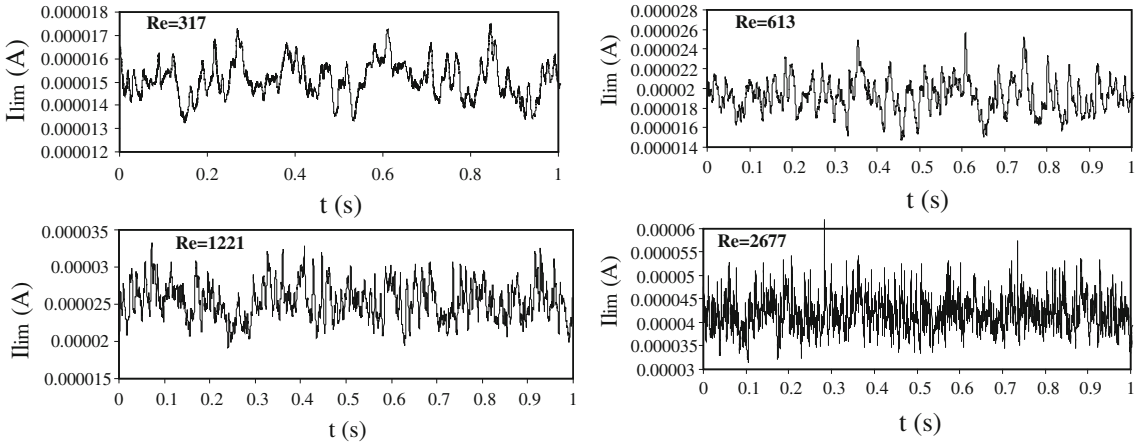

Fig. 2 Time-traces of the current recorded on electrode M15 for different Reynolds numbers

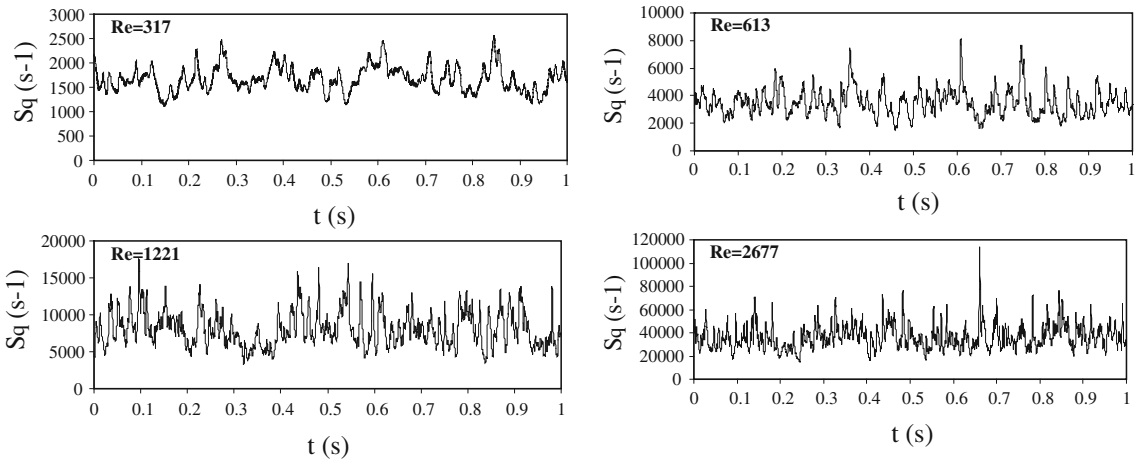

Fig. 3 Time-traces of the quasi-steady wall shear rate recorded on electrode M15 for different Reynolds numbers

where $f(t)$ is a general time function that takes into account a time delay of the wall shear rate. The solution of the diffusion–convection equation in the entire mass boundary layer leads to the following general expression of the time history of the wall shear rate, $s(t)$:

$$s(t) = s_q(t) + \frac{2}{3} t_0 \left(\frac{\partial s_q}{\partial t} \right) \tag{6}$$

where t_0 is the characteristic time of the probe, defined as a dynamic behavior parameter of the electrodiffusion probe, i.e.:

$$t_0(t) = 0.426 d_e^{2/3} D^{-1/3} s_q(t) \tag{7}$$

This relationship has been used by several authors in different flow configurations (Labraga et al. 2002; Tihon et al. 2003); they found it relevant in unsteady flow conditions, even when compared with the inverse method (Rehimi et al. 2006).

The time series of the corrected wall shear rate at the M15 electrode is shown in Fig. 4 for different Reynolds numbers. The signals are marked by unsteady events and distinguished by greater amplitudes as the Reynolds number increases. These intermittent phenomena, associated with a well-organized sequence of large-scale motions, have been previously analyzed in detail (Huchet et al. 2008a).

2.2.2 *Power density spectrum of the current*

A comparison of the transfer function with Sobolik's correction can be performed using a frequency representation of signals. The signal processing procedure will be provided in this subsection; it covers the steps typically applied when obtaining an experimental characterization of turbulent flow from either passive scalars or one of the velocity components.

The unsteady variations in current measured by the microelectrodes correspond to fluctuations in the concentration of active species within the diffusive boundary layer. These fluctuations are strongly correlated with flow

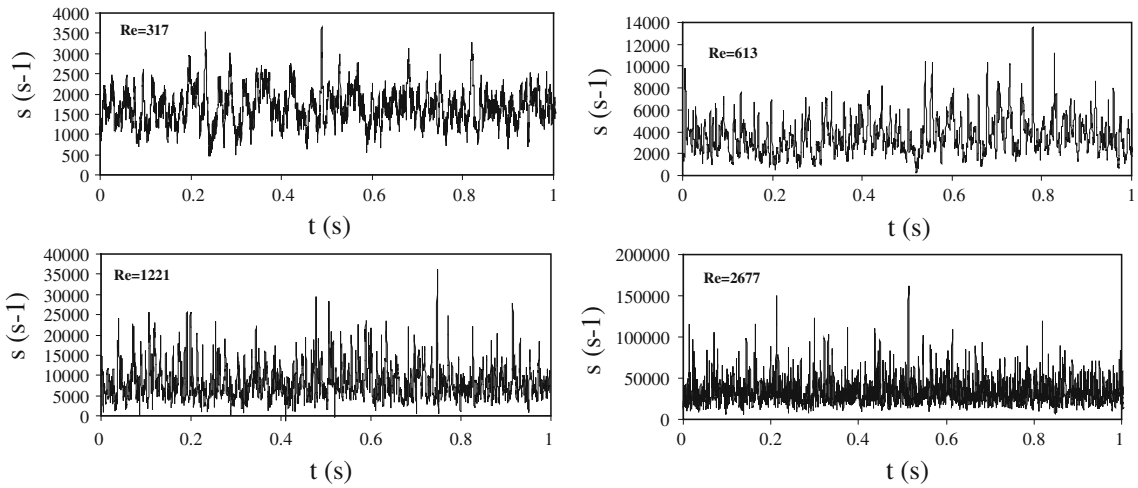

Fig. 4 Time-traces of the corrected wall shear rate recorded on electrode M15 for different Reynolds numbers

fluctuations occurring both inside and outside the hydrodynamic boundary layer. The recording of a random signal such as the current requires a one-dimensional Fourier transform in order to obtain the energy distribution within the frequency domain. Moreover, it offers a physical meaning for the temporal signal that appears as noise. The present methodology has been inspired from the literature (Max 1985), and its first step consists of extracting the fluctuating value, $i(t)$, from the recorded signal, $I_{\text{lim}}(t)$, as defined by:

$$I_{\text{lim}}(t) = \overline{I_{\text{lim}}} + i(t) \tag{8}$$

The resulting signal is divided into N blocks, each of them having the same number of points, N_e. These blocks all display a 50% overlap. Each part of the signal, $i(t)_N$, is processed independently. This averaging method makes it possible to remove perturbations (such as ambient noise or electromagnetism wave) and hence preserve the representation of physical phenomena. N_e depends on the temporal resolution of the particular phenomenon under study. The sampling frequency is adjusted as a function of turbulence level (Huchet et al. 2007) for the purpose of describing all physical information over the various sub-ranges of the spectra. The scanned scales of energy therefore include those containing eddies as well as the smallest scale, which depends on the diffusivity ratio.

On the other hand, each block is multiplied by a temporal window of size N_e; this function allows eliminating the lobe phenomenon that arises whenever a Fourier transform is applied to a finite signal.

The truncation effect can then be reduced by introducing Hanning's window, which is defined by:

$$F_{\text{ha}}(t) = 0.5 \times \left(1 + \cos\frac{\pi t}{N_e}\right) \tag{9}$$

The power spectral density of the current, $W_{ii}(f)_N$, is then obtained by discrete Fourier transform of the focused parts of the signal; their integration gives rise to the PSD, W_{ii}:

$$W_{ii}^{i} = \int_0^N (i(t)_N \times F_{\text{ha}}(t)) \times \exp(-j2\pi ft)\mathrm{d}t \tag{10}$$

$$W_{ii} = \frac{\sum_{i=1}^{N} W_{ii}^{i}}{N} \tag{11}$$

The same procedure has been applied again in order to compare the electrochemical transfer function and the corrected solution according to the methodology presented in Fig. 5.

Figure 6 shows the PSD of the current, W_{ii}, for a wide range of Reynolds numbers ($317 < Re < 3{,}535$) at three positions in the network, i.e., the system inlet (electrode M34), the middle section after a crossing (A28), and near the system outlet (M15). As considered previously by Tennekes and Lumley (1972) and proven more recently experimentally and numerically by other authors (Campbell and Hanratty 1983; Labraga et al. 2002, Calmet and Magnaudet 1997), the spectrum cascades appearance correspond quite well to the standard concentration spectra of the electrochemical species dynamically mixed within the hydrodynamic boundary layer. Coherent structures and bursting phenomena coexist in the near-wall region and control the mass transfer fluxes in the viscous sub-layer. Regarding the microelectrodes located in the non-established flow area (M34 to A28), one can observe from $Re = 317$ a first peak at $f = 5$ Hz which remains insignificant, energetically speaking, for M34 probe while probe A28 exhibits a plateau in the low-frequency area ($2 > f(\text{Hz}) > 50$) corresponding to the first instabilities. From $Re = 613$, spectra exhibit an inertial sub-range

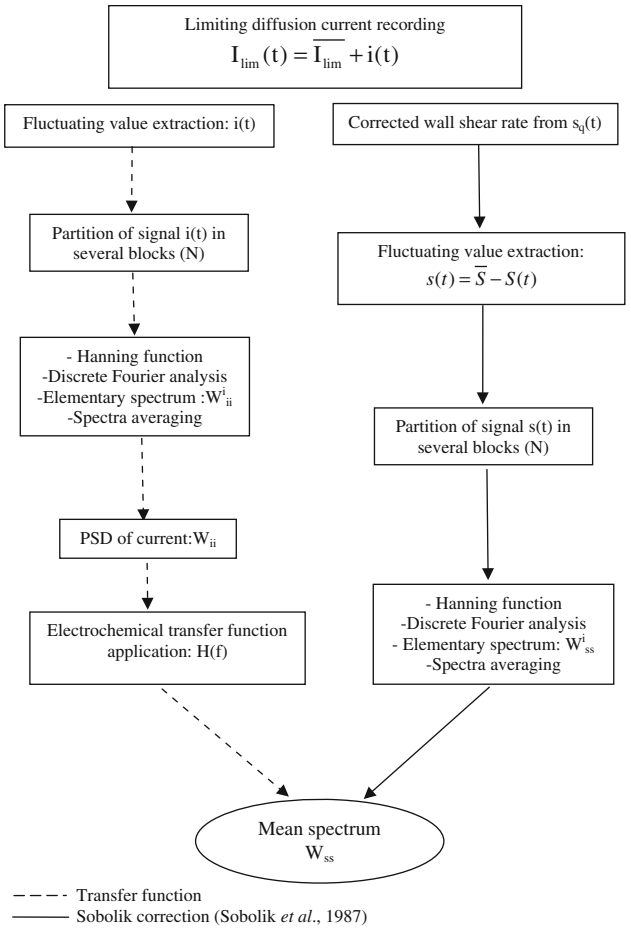

Fig. 5 Different steps of the signal processing. *Dashed with dotted line* transfer function and *solid line* Sobolik correction (Sobolik et al. 1987)

starting from $f = 50$ Hz at lower Reynolds numbers until $f = 150$ Hz for the higher Reynolds number. The typical spectra decline with a slope equal to f^{-4}. In fully-developed flow (M15 location) and whatever the Reynolds numbers, the spectra are characterized by a low-frequency plateau followed by a downward slope reaching f^{-4} over a large range of frequencies $f = [50–3{,}500$ Hz]. Fluctuations positioned in the high frequency range ($f = 1{,}489$ Hz to $f = 3{,}335$ Hz) of the spectra are attributed to the parasite noise linked to the equipments required in the electrochemical-flow experiments (pumps, acquiring system, electromagnetical interference).

2.2.3 *Transfer function and comparison with Sobolik's correction*

The transfer function, $H(f)$, serves to determine the power spectral density (PSD) of wall shear rate fluctuations, $W_{SS}(f)$, based on the PSD of instantaneous current fluctuations, $W_{ii}(f)$. The frequency response of electrochemical probes is taken into account in order to restore the shear rate fluctuation spectrum from current fluctuations according to the following relationship:

$$W_{ss}(f) = W_{ii}(f)/|H(f)|^2 \tag{12}$$

A correct use of Eq. 12 requires the two following conditions:

1. the transfer function must be accurately known over the entire frequency range;
2. the homogeneity condition with time-dependent fluctuations must be uniform over the entire probe surface.

Several expressions have been proposed for the transfer function. With circular probes, we have selected the following equation from Nakoryakov et al. (1986):

$$H(\sigma) = H(0)\left(1 + 0.049\sigma^2 + 0.0006\sigma^4\right)^{-1/2} \quad \text{for } 1 < \sigma < 6 \tag{13}$$

$$H(\sigma) = H(0)\frac{4.416}{\sigma}\left[1 - \frac{1.7}{\sqrt{\sigma}} + \frac{1.44}{\sigma}\right]^{1/2} \quad \text{for } \sigma > 6 \tag{14}$$

with σ defined as a dimensionless frequency:

$$\sigma = 2\pi f\left(\frac{d_e^2}{D\overline{s^2}}\right)^{1/3} \tag{15}$$

and the normalized transfer function when the frequency tends to zero:

$$|H(0)| = \frac{1}{3}\frac{\overline{I_{lim}}}{\overline{s}} \tag{16}$$

The PSD of the wall shear rate fluctuations obtained with this electrochemical transfer function is presented in Fig. 7 and compared with the PSD calculated from the corrected wall shear rate fluctuations.

Each spectrum is typically characterized by a plateau located at low frequencies and a decrease in the high-frequency area. When examining typical spectra, the slope observed in the latter part differs depending on the probe position within the network. The logarithmic trends are characterized by a slope that varies of the classical reference $f^{-5/3}$. It must be pointed out in the present case that the first hypothesis is not being satisfied: the transfer function is not capable of appropriately represent the entire range of high fluctuations since a cutoff frequency appears in each spectrum ($500 < f(\text{Hz}) < 1{,}500$).

This remark confirms those previously reported by Huchet et al. (2008a) concerning the spatial and temporal intermittency phenomena encountered within the mini-channel network, where fluctuations amplitudes of the shear rate are high relative to the time-averaged shear rate values. The linearization theory of the transfer function is therefore not valid, and the direct correction of

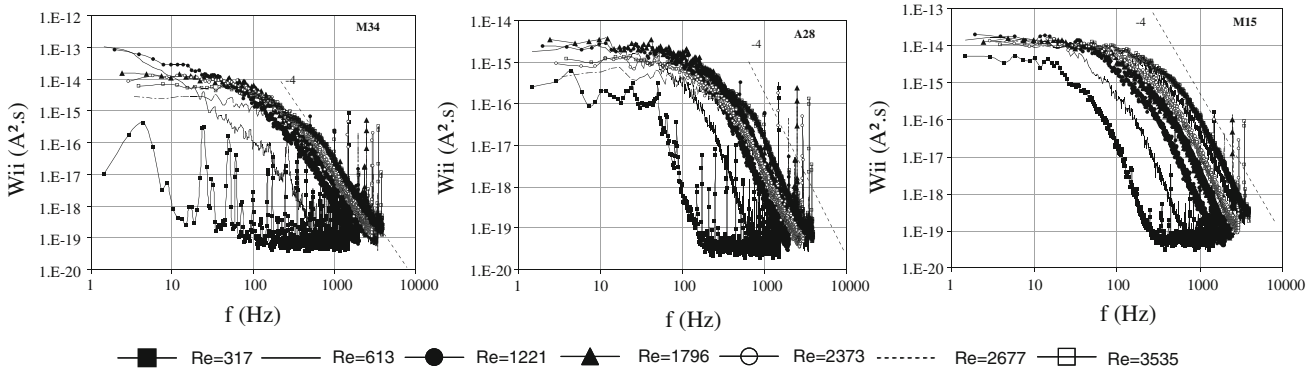

Fig. 6 PSD of the limiting current fluctuations for three electrodes for different Reynolds numbers. *Filled square Re* = 317; *solid line Re* = 613; *filled circle Re* = 1,221; *filled triangle Re* = 1,796; *open square Re* = 2,373; *dashed with dotted line Re* = 2,677; *open square Re* = 3,535

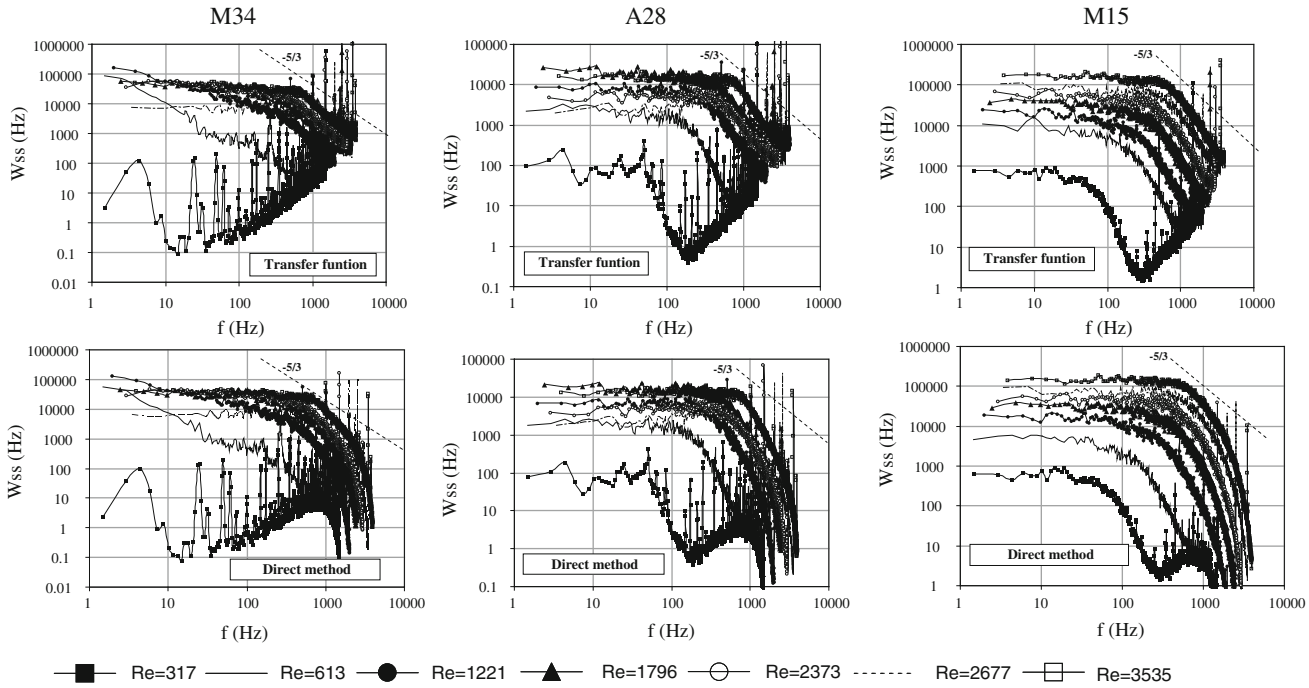

Fig. 7 Comparison of the PSD of the fluctuations of the wall shear rate between transfer function method and Sobolik's solution (direct solution) for three working microelectrodes and several Reynolds numbers. *Filled square Re* = 317; *solid line Re* = 613; *filled circle Re* = 1,221; *filled triangle Re* = 1,796; *open square Re* = 2,373; *dashed with dotted line Re* = 2,677; *open square Re* = 3,535

electrochemical signals seems to be a more attractive method for solving the issue of dynamic electrochemical probe behavior.

The shape of the PSD of corrected shear rate at the wall is similar to that calculated by the transfer function over the frequency range corresponding to intermediate and large flow structures ($1 < f(\text{Hz}) < 1{,}000$). Above a frequency level equal to $f \approx 1{,}000$ Hz, the PSD of the corrected wall shear rate yields certain information in the dissipative area of the spectra that would be impossible to obtain with the method based on the transfer function. It may be noticed that the level of fluctuations of the wall shear rate calculated using the transfer function remains correct since this part of the spectra does not influence the integrated PSD value. Nevertheless, it is important to select the correction method of Sobolik et al. (1987) in order to analyze mixing phenomena from the electrochemical method, since flow structures associated with the micromixing phenomena, which provide the best reaction conditions, are located in the dissipative part of the spectra. In the following section, we will thus apply this method to the hydrodynamic study inside micromixers.

3 Spectral analysis of wall shear rate fluctuations inside micromixers

3.1 The micromixer apparatus

The micromixers under study are operated with two flow configurations: crossing-flow and impinging-flow, respectively (shown in Figs. 8, 9). An initial study (Huchet et al. 2008c) was performed for the purpose of determining the mean wall shear rate from eight microelectrodes flush-mounted on the wall. The physical and chemical properties of the electrochemical solution implemented in this work are summarized in Table 1. Good agreement with the numerical wall shear rate, calculated using computational fluid dynamics under steady-state conditions, was obtained at the outset. The electrochemical technique has proven its ability for the determination of the establishing length of the flow in micromixers, along with its advantages for the scale design of such systems. Based on these primary results, we will now use Sobolik's solution (Sobolik et al. 1987) in order to characterize the flow under unsteady conditions from the spectral analysis and, in particular, to detect the flow structures responsible for mixing at the various flow scales. A polarization voltage equal to −0.7 V is applied between circular anode located at the outlets of the microsystems and the working microelectrodes. A home built electrodiffusion analyzer is used in order to record the voltage after conversion and amplification of the measured current. The acquired data are treated with a sampling frequency equal to 6 kHz during 30 s. For each measurement, a set of 18,000 data is considered as being sufficiently representative. Each set of data involves a number of blocks equal to $N = 174$ and corresponding to 2,048 data. Each window is 50% overlapped in the frame of the averaging of the PSD according to the procedure given in Fig. 5.

The experimental cell, as shown in Fig. 10a, is composed of two PMMA plates, respectively the "bottom" and the "cover" screwed together. The "bottom" plate is one of the two available where microchannels have been milled so as to test two hydraulic diameters. For one plate, the channels have a rectangular Section 500 µm wide and 2,500 µm deep, yielding a hydraulic diameter, d_h, equal to 833 µm (see Table 2). For the second plate, the channels are characterized by a square section 500 µm on a side ($d_h = 500$ µm). The "cover" plate supports eight microelectrodes acting as cathodes in the electrical circuit; they are made from platinum wires and flush-mounted on the wall. These probes are positioned along coordinates (x, y), whose origin is defined at the branch entrance. A dimensionless positioning, x_p (x/d_h), is based on the ratio of the distance between branch entrance and center of the microelectrode to the hydraulic diameter. The spectral

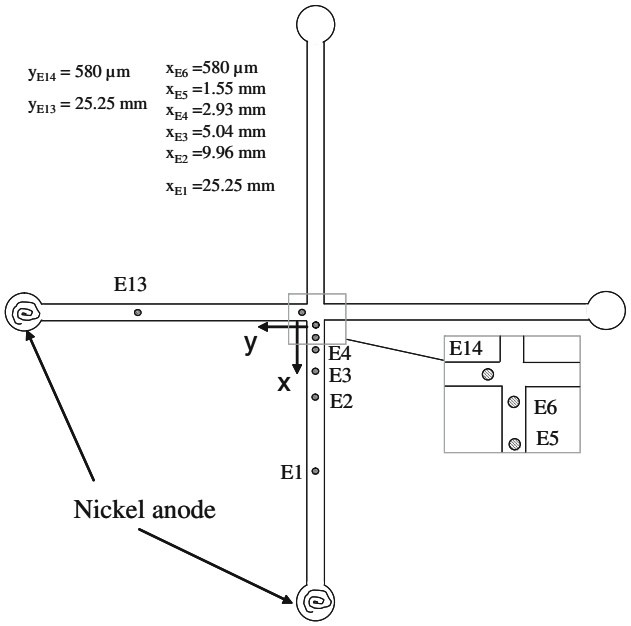

Fig. 8 Position of the microelectrode in flow microcell

analysis presently focuses on three electrodes and for a large range of Reynolds numbers calculated from the hydraulic diameter and the mean velocity in the microchannel, U, i.e.,:

- E6 and E5, which are respectively located at the dimensionless positions such that $x_{pE6} = 0.7$ and $x_{pE5} = 1.9$ for $d_h = 833$ µm, and that $x_{pE6} = 1.2$ and $x_{pE5} = 3.1$ for $d_h = 500$ µm. These electrodes are the closest to the crossing and are expected to provide information regarding the impact of the crossing on flow-mixing structures;
- E14 is located at the dimensionless positions $y_{pE14} = -0.7$ for $d_h = 833$ µm and $y_{pE14} = -1.2$ for $d_h = 500$ µm. Depending on the flow configuration, this electrode is located in the inlet branch of the crossing micromixer (impinging-flow) or in the second outlet branch (crossing-flow).

3.2 Crossing-flow pattern

Figure 11 illustrates the spectral analysis performed on wall shear rate fluctuations recorded from three microelectrodes located in the outlet branches, respectively E6, E5, and E14, according to the two studied cross-sections.

1.

$d_h = 833\,\mu m - \gamma = 0.2$

The spectra appearance of E6 and E14 are not exactly identical because of the location of the two microelectrodes. As shown by image analysis in Fig. 10b,

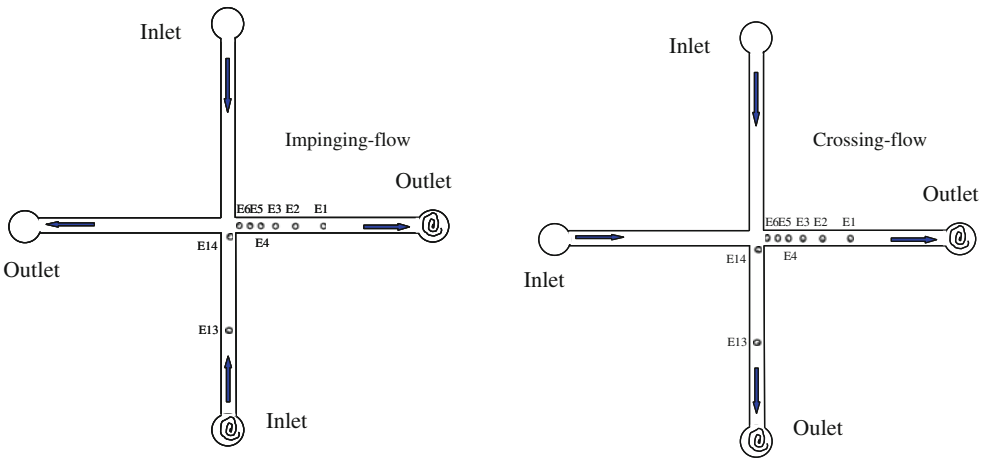

Fig. 9 Scheme of the pattern flows: impinging-flow and crossing-flow

Table 1 Characteristics of the microsystems

d_h (μm)	Aspect ratio γ	Materials	Electrodes types	*Re* range	Inlet pressure delivering (bar)
833	0.2	PMMA	Platinum wire	25–1,150	~0.5
500	1	PMMA	Platinum wire	70–3,350	~2

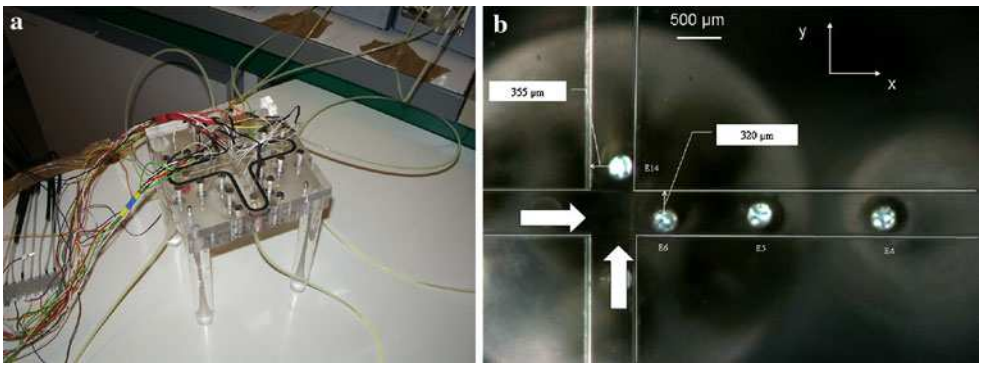

Fig. 10 **a** Experimental Plexiglas cell. **b** View of the microprobes at the crossing microchannels

their respective positions are not exactly symmetric with regard to the center line of the microchannel. The E5 spectrum is characterized by a peak identified at $f = 200$ Hz for $Re = 1{,}165$, which is representative of the vortices previously identified in crossing minichannel networks (Huchet et al. 2008a), as well as by two declining trends in the slope ranging from $f^{-5/3}$, the classical Kolmogorov reference, to f^{-3}.

2.

$d_h = 500\,\mu\text{m} - \gamma = 1$

With $d_h = 500$ μm, as opposed to spectra derived from classical flow inside macro- or millidevices, the spectra shape is characterized by a decrease in the low-frequency area with a slope varying between $-1/3$ and -1, depending on both probe position and hydraulic diameter. These multi-scale characteristics can be attributed to the confinement effect, whereby wall friction is predominant in the microchannels. The input energy generated by the pump inside the micromixer is thus dissipated by wall effects, which involves an energy drop in the low-frequency domain of the spectra.

A distinct second declining trend in the spectra appears above a value of $f = 1{,}000$ Hz, as characterized by a logarithmic trend equal to f^{-4} for $1{,}000 < Re < 3{,}333$. This finding can be explained by a flow confinement that serves to enhance the micromixing phenomena. The finer flow scales associated with the so-called Kolmogorov scales indeed act as a mixing effect at microscales before molecular diffusion. The observed spectral evolution (f^{-4} slope decay) is representative of the viscous-diffusive subrange, where molecular diffusion becomes effective due to variance in the local dissipation of concentration. This evolution corresponds quite well to the shape of the PSD of

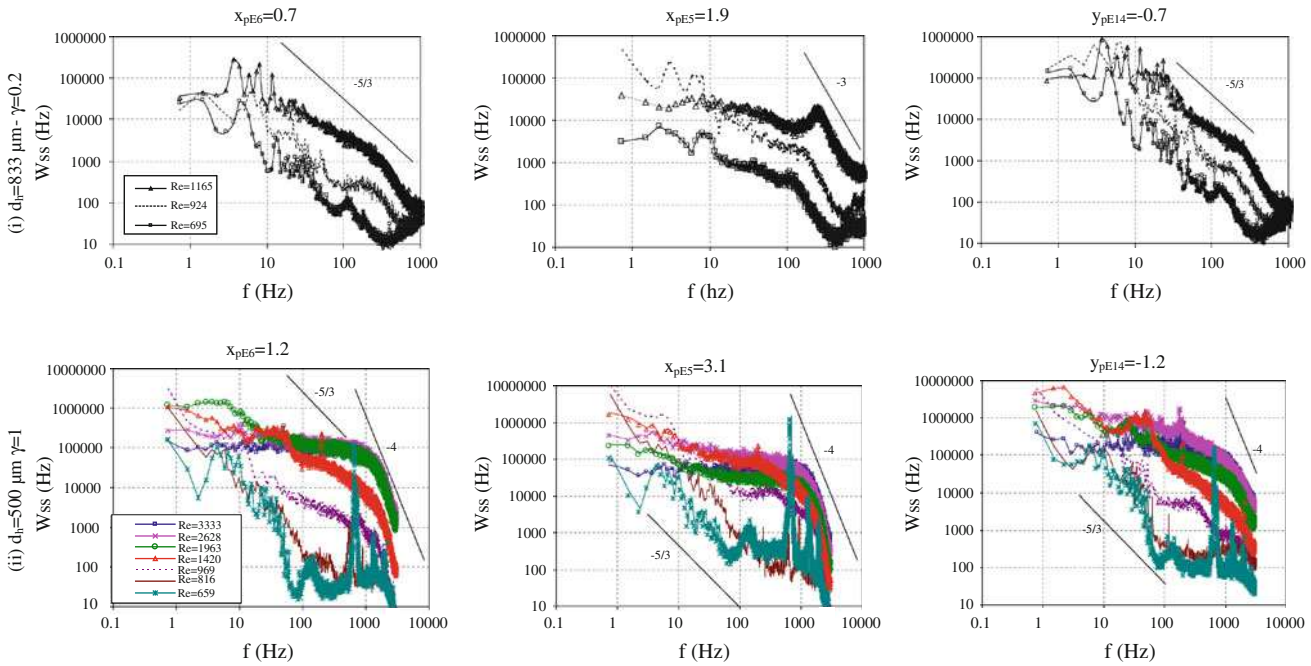

Fig. 11 Comparison of the PSD of the wall shear rate fluctuations obtained with two aspect ratios. Case of a micromixer used with the crossing-flow configuration

the current representing classical fluctuations of electrochemical species concentration, as previously indicated in Fig. 6.

3.3 Impinging-flow pattern

Figure 12 presents the PSD of wall shear rate fluctuations calculated at three electrodes both located before (E14) and after (E6 and E5) the impingement of fluid streams at the crossing according to the two studied cross-sections.

1.

$d_h = 833\,\mu m - \gamma = 0.2$

For each position, a large decrease in spectra occurs from the low-frequency part varying according to the probes' position. For example, at E6 and $Re = 287$, the spectrum decreases until $f = 30$ Hz then exhibits a plateau containing several peaks ($f = 328$ Hz) before falling down toward the high frequency domain. This observation reveals a viscous-convective sub-range, as characterized by large eddies advected in the streamwise direction, whose fluctuations are reduced by the strain rate field and cascades toward smaller eddies. The second part of the PSD is similar to that obtained in the 500-µm microchannel characterized by a slope close to −4. By focusing on the respective positions of electrodes E5 and E6, where the streams are subjected to strong shearing and stretching, the viscous-diffusive sub-range appears earlier than in spectra involved in a crossing-flow pattern, as previously described in Sect. 3.2.

2.

$d_h = 500\,\mu m - \gamma = 1$

For a hydraulic diameter equal to 500 µm, the spectra calculated from E14 ($y_{pE14} = -1.2$) at $Re = 511$ exhibits a first plateau until $f = 150$ Hz, then decrease until $f = 380$ Hz within a narrow frequency band until the decreasing toward the low energy part.

In the output branches, this impinging-flow effect increases the spectra level, especially at $Re = 173$, for which eddy formation is sufficient to disrupt output flow and induce mixing structures. This phenomenon has already been observed by several authors for the T-shaped configuration in this flow regime (Bothe and Warnecke 2006; Hoffmann et al. 2006; Kockmann et al. 2006; Soleymani et al. 2008). Above $Re = 1{,}000$, the flow regime in straight microchannels has only been investigated by Natrajan and Christensen (2009) using µPIV. Downstream of fluid impingement, the formation of a wake composed of complex flow structures was simulated by Lui et al. (2009) until $Re = 1{,}013$. These last authors found an inadequate level of agreement between µPIV and CFD simulation. As the low-frequency camera sampling filters the velocity fluctuations, the authors recommend the large-eddy simulation approach for this type of microflow

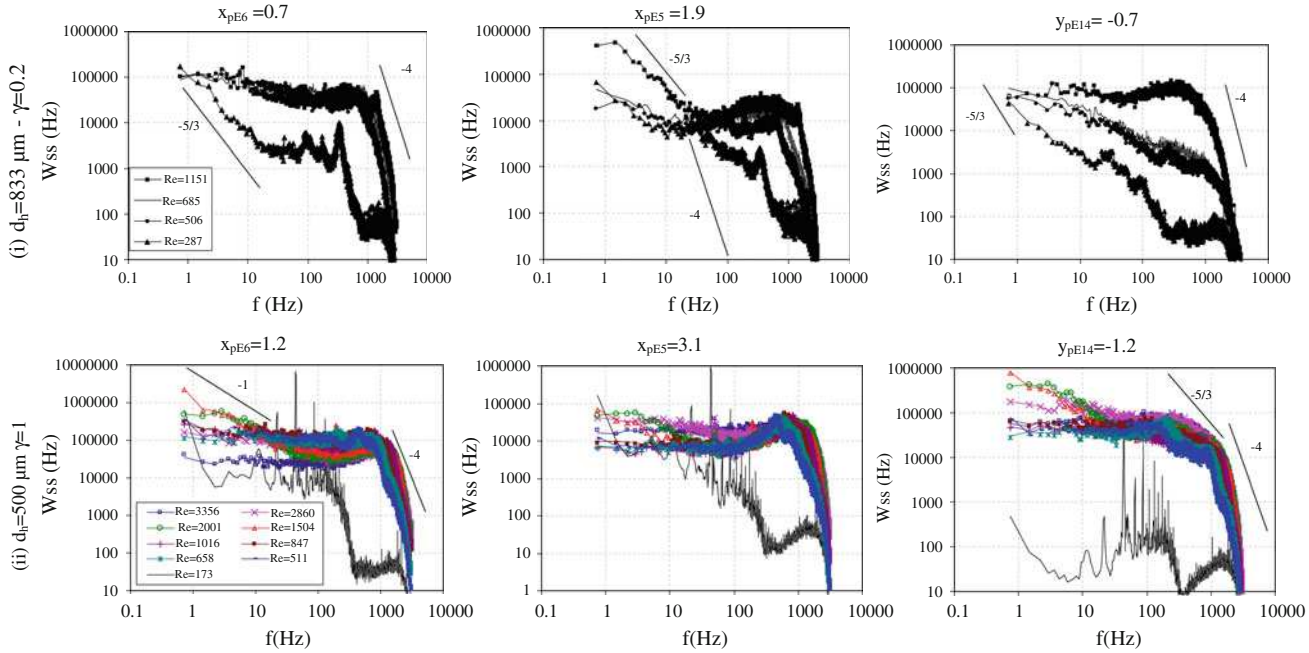

Fig. 12 Comparison of the PSD of the wall shear rate fluctuations obtained with two aspect ratios. Case of a micromixer used with the impinging-flow configuration

Table 2 Physical and chemical properties of the electrochemical solution

Solution	ρ (kg m^{-3})	μ (Pa s)	D (m^2 s^{-1})
$[Fe_3(CN)_6] = 0.005$ M $[Fe_4(CN)_6] = 0.025$ M	1,060	$1.049.10^{-3}$	$5.83.10^{-10}$

analysis in order to solve the entire range of flow structures, from the integral scale until the Kolmogorov scale before diffusion by the Batchelor scale. To the best of our knowledge, the present experimental data, as analyzed through shear rate fluctuation spectra at the wall, are the first set of this kind to exhibit the actual unsteady nature of impinging microflow patterns.

According to the spectra shown in Fig. 12 for E6 and E5 positions, several peaks appear that correspond to a detachment of vortices in the downstream part of the impingement stream. Eddies associated with such detachment are characterized by a frequency detachment, F, such as reported in Table 3 for the E5 electrode. Above $Re = 1{,}016$, these peaks are located in the high-frequency domain of the spectra. The friction velocity, $U\tau = (\mu\bar{s}/\rho)^{0.5}$, calculated from the mean wall shear rate is plotted in Fig. 13 at every position of the outlet branches of the impingement micromixer. The high values observed close to the outlet at 1.2 d_h and 3.1 d_h confirm the strong shearing and stretching induced by the vortices deduced from the PSD. At 10.1 d_h, the velocity friction rises ($U_\tau = 0.78$ m.s^{-1} at $Re = 2{,}680$) exhibiting an enhancement of the local wall mass transfer then reaching a plateau until the last electrochemical probe located at 50.5 d_h.

4 Conclusion

Sobolik's method has been performed to determine the power spectra density (PSD) of wall shear rate fluctuations within a network of crossing minichannels (side length of 1.5 mm). This method was applied to the flow in crossing microchannels with dimensions of 833 and 500 µm.

Table 3 Recapitulative of the flow characteristics at $x/d_h = 3.1$ in impinging type micromixer of aspect ratio equal to 1 and $d_h = 500$ µm

U (m s^{-1})	1.01	1.3	1.67	2.01	2.97	3.95	5.29	6.63
Re	511	658	847	1,016	1,504	2,001	2,680	3,356
$\bar{s}$(s^{-1})	100,700	132,680	183,440	237,510	382,460	547,180	808,100	107,4500
F_{E5} (Hz)	443	542	619	720	769	985	849	748

Frequency detachment of the vortices from psd and mean wall shear rate

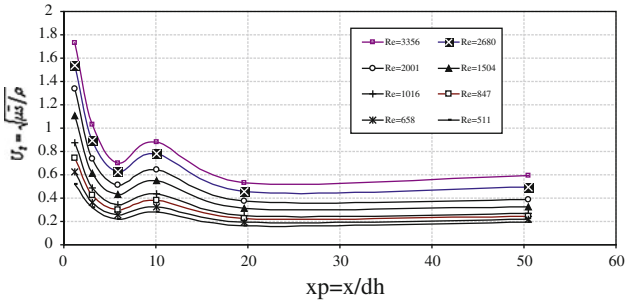

Fig. 13 Friction velocity along the outlet branches of the impingement micromixer of aspect ratio equal to 1 and $d_h = 500$ μm

Several flow patterns were explored in order to reveal the flow footprints inside micromixers as well as the influence of channel size on both wall turbulence properties and mixing analysis at the microscales.

The spectral analysis of wall shear rate fluctuations recorded from non-intrusive electrochemical probes appears to be suitable for complex confined flows such as those encountered in micromixer applications. Even if the flow scales were averaged over the probe surface area, the evolution in spectra would reveal unusual characteristics that differ from those detected using measurements performed with the same electrochemical technique in classically sized channels. The narrower channel dimension induces different PSD shapes, especially at higher frequencies. This phenomenon can be explained quite well by turbulence theory. The confinement effects delay turbulence properties toward the low-frequency part depending on the characteristic sizes of the channels:

- At 1.5 mm, the PSD of the current (or concentration) evolves with f^{-4}, which corresponds to the viscous-diffusive sub-range belonging to the concentration spectra. The PSD of the velocity gradient is standard and characterized by a classical plateau followed by a drop that varies with the classical reference $f^{-5/3}$.
- At 833 μm, while the flow is developed, the PSD of the wall shear rate follows a viscous-convective sub-range. Once vortices start to occur (impinging micromixer), the PSD gives rise to an evolution with f^{-4}, which corresponds to the viscous-diffusive sub-range where eddies enhance mixing at the microscales.
- Lastly, at a size of 500 μm and regardless of the upstream flow characteristics, the measured PSD of the velocity gradient evolves with f^{-4} in a viscous-diffusive sub-range. The dissipative phenomena increase with a decrease in channel size: the turbulence laws are not being respected.

Next issues are to reduce the size of the microelectrodes in order to increase the accuracy in the determination of the high-frequency fluctuations of the power spectra density. According to the literature, a value of $L^+ = 20$ (with $L^+ = \rho d_e U_\tau / \mu$) is expected to overcome the spatial cutoff frequency of the microelectrodes and capture the smallest scales of the mixing in the near-wall vicinity of the microsystems.

References

Bothe D, Warnecke HJ (2006) Fluid mixing in a T-shaped micromixer. Chem Eng Sci 61:2950–2958

Brandner JJ, Anurjew E, Bohnn L, Hansjosten E, Henning T, Schygulla U, Wenka A, Shubert K (2006) Concepts and realization of microstructured heat exchangers for enhanced heat transfer. Exp Therm Fluid Sci 30:801–809

Calmet I, Magnaudet J (1997) Large-eddy simulation of high-Schmidt number mass transfer in a turbulent channel flow. Phys Fluids 9:438–455

Campbell JA, Hanratty TJ (1983) Turbulent velocity fluctuations that control mass transfer to a solid boundary. AIChE J 28(2): 215–221

Commenge JM, Falk L, Corriou JP, Matlosz M (2004) Intensification des procédés par microstructuration. C R Physique 5:597–608

Deslouis C, Gil O, Tribollet B (1990) Frequency response of electrochemical sensors to hydrodynamic fluctuations. J Fluid Mech 215:85–100

Gavrilidis A, Angeli P, Cao E, Yeong KK, Wan YSS (2002) Technology and applications of microengineered reactors. Chem Eng Res Des A 80:3–30

Hanratty TJ, Campbell JA (1983) Measurement of wall shear stress. In: Goldstein RJ (ed) Fluid mechanics measurements. Hemisphere, New York, p 559

Hansen C, Quake SR (2003) Microfluidics in structural biology: smaller, faster… better. Curr Opin Struct Biol 13:538–544

Hessel V, Löwe H, Schönfeld F (2005) Micromixers—a review on passive and active mixing principles. Chem Eng Sci 60:2479–2501

Hoffmann M, Schluter M, Rabiger N (2006) Experimental investigation of liquid-liquid mixing in T-shaped micro-mixers using μ-LIF and μ-PIV. Chem Eng Sci 61:2968–2976

Huchet F, Comiti J, Tihon J, Montillet A, Legentilhomme P (2007) Electrodiffusion diagnostics of the flow and mass transfer inside a network of crossing minichannels. J Appl Electrochem 37:49–55

Huchet F, Comiti J, Legentilhomme P, Solliec C, Legrand J, Montillet A (2008a) Multi-scale analysis of hydrodynamics inside a network of crossing minichannels using electrodiffusion method and PIV measurements. Int J Heat Fluid Flow 29:1411–1421

Huchet F, Comiti J, Legentilhomme P, Bennadji H (2008b) Mixing characterization and energetic dissipation in different networks of crossing minichannels. Chem Eng Res Des 86:1135–1142

Huchet F, Havlica J, Legentilhomme P, Montillet A, Comiti J, Tihon J (2008c) Use of electrochemical microsensors for hydrodynamics study in crossing microchannels. Microfluid Nanofluid 5:55–64

Kjeang E, Roesch B, McKechnie J, Harrington DA, Djilali N, Sinton D (2007) Integrated electrochemical velocimetry for microfluidic devices. Microfluid Nanofluid 3:403–416

Kockmann N, Kiefer T, Engler M, Woias P (2006) Convective mixing and chemical reactions in microchannels with high flow rates. Sensors Actuat B 117:495–508

Labraga L, Lagraa B, Mazouz A, Keirsbulck L (2002) Propagation of shear-layer structures in the near-wall region of a turbulent boundary layer. Exp Fluids 33:670–676

Lévêque MA (1928) Les lois de la transmission de la chaleur par convection. Ann Mines 12:201

Lui Y, Olsen MG, Fox RO (2009) Turbulence in a microscale planar confined impinging-jets reactor. Lab Chip 9:1110–1118

Max J (1985) In: Méthodes et techniques de traitement du signal et applications aux mesures physiques, 4th edn. Masson, Paris

Mokrani O, Bourouga B, Castelain C, Peerhossaini H (2009) Fluid flow and convective heat transfer in flat microchannels. Int J Heat Mass Transf 52:1337–1352

Morini GL (2004) Single phase convective heat transfer in microchannels: a review of experimental results. Int J Therm Sci 43:631–651

Nakoryakov VE, Budukov AP, Kashinsky ON, Geshev PI (1986) In: Gasenko VG (ed) Electrodiffusion method of investigation into the local structure of turbulent flows. Novosibirsk

Natrajan VK, Christensen KT (2009) Structural characteristics of transition to turbulence in microscales capillaries. Phys Fluids 21:034104

Rehimi F, Aloui F, Ben Nasrallah S, Doubliez L, Legrand J (2006) Inverse method for electrodiffusional diagnostics of flow. Int J Heat Mass Transf 49:1242–1254

Reiss LP, Hanratty TJ (1963) An experimental study of the unsteady nature of the viscous sublayer. AIChE J 8:154–160

Saber M, Commenge JM, Falk L (2009) Rapid design of channel multi-scale networks with minimum flow maldistribution. Chem Eng Process 48(3):723–733

Saber M, Commenge JM, Falk L (2010) Microreactor numbering-up in multi-scale networks for industrial-scale applications: impact of flow maldistribution on the reactor performances. Chem Eng Sci 65(1):372–379

Schrott W, Svoboda M, Slouka Z, Šnita D (2009) Metal electrodes in plastic microfluidic systems. Microelectron Eng J 86:1340–1342

Sharp KV, Adrian RJ (2004) Transition from laminar to turbulent flow in liquid filled microtubes. Exp Fluids 36:741–747

Sobolik V, Wein O, Cermak J (1987) Simultaneous measurement of film thickness and wall shear stress in wavy flow of non-Newtonian liquids. Coll Czech Chem Commun 52:913–928

Soleymani A, Kolehmainen E, Turunen I (2008) Numerical and experimental investigations of liquid mixing T-type micromixers. Chem Eng J 135:219–228

Stroock AD, Dertinger SKW, Ajdari A, Mezi I, Stone HA, Whitesides GM (2002) Chaotic mixer for microchannels. Science 295:647–651

Tennekes H, Lumley JL (1972) A first course in turbulence, chap. 8. MIT Press, Cambridge, p 286

Tihon J, Tovchigrechko V, Sobolik V, Wein O (2003) Electrodiffusion of the near-wall reversal in liquid films at the regime of solitary waves. J Appl Electrochem 33:577–587